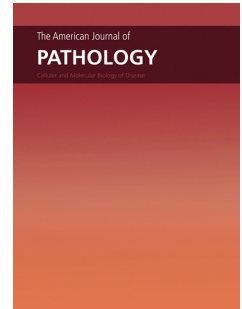


Accepted Manuscript



Intrinsic Bone Defects in Cystinotic Mice

Giulia Battafarano, Michela Rossi, Laura Rita Rega, Gianna Di Giovamberardino, Anna Pastore, Matteo D'Agostini, Ottavia Porzio, Nathalie Nevo, Francesco Emma, Anna Taranta, Andrea Del Fattore

PII: S0002-9440(18)30964-7

DOI: <https://doi.org/10.1016/j.ajpath.2019.01.015>

Reference: AJPA 3091

To appear in: *The American Journal of Pathology*

Received Date: 15 November 2018

Revised Date: 9 January 2019

Accepted Date: 24 January 2019

Please cite this article as: Battafarano G, Rossi M, Rega LR, Di Giovamberardino G, Pastore A, D'Agostini M, Porzio O, Nevo N, Emma F, Taranta A, Del Fattore A, Intrinsic Bone Defects in Cystinotic Mice, *The American Journal of Pathology* (2019), doi: <https://doi.org/10.1016/j.ajpath.2019.01.015>.

This is a PDF file of an unedited manuscript that has been accepted for publication. As a service to our customers we are providing this early version of the manuscript. The manuscript will undergo copyediting, typesetting, and review of the resulting proof before it is published in its final form. Please note that during the production process errors may be discovered which could affect the content, and all legal disclaimers that apply to the journal pertain.

Intrinsic bone defects in cystinotic mice

Giulia Battafarano, Dr¹; Michela Rossi, Dr¹; Laura Rita Rega, PhD²; Gianna Di Giovamberardino, Dr³; Anna Pastore, PhD⁴; Matteo D'Agostini, Dr⁵; Ottavia Porzio, MD⁵⁻⁶; Nathalie Nevo, PhD⁷; Francesco Emma, MD, PhD²⁻⁸; Anna Taranta, PhD*² and Andrea Del Fattore, PhD*¹

¹Bone Physiopathology Group, Multifactorial Disease and Complex Phenotype Research Area, Bambino Gesù Children's Hospital, Rome, Italy; ²Laboratory of Nephrology, Division of Genetic and Rare Diseases, Bambino Gesù Children's Hospital, Rome, Italy; ³Research Laboratories, Bambino Gesù Children's Hospital, Rome, Italy; ⁴Laboratory of Molecular Genetics and Functional Genomics, Division of Genetic and Rare Diseases, Bambino Gesù Children's Hospital, Rome, Italy; ⁵Clinical Laboratory, Bambino Gesù Children's Hospital, Rome, Italy; ⁶Department of Experimental Medicine, University of Rome Tor Vergata, Rome, Italy; ⁷INSERM U1163, Université Paris Descartes, Institut Imagine, Hôpital Necker Enfants Malades, 75015, Paris, France; ⁸Division of Nephrology, Department of Pediatric Subspecialities, Bambino Gesù Children's Hospital, Rome, Italy.

Number of text pages: 26

Number of tables: 5

Number of figures: 8

Short running head: Reduced bone mass in Cystinosis

Funding: Supported by Cystinosis Research Foundation (grant #CRFS-2015-006) to A.T. and A.D.F., and the Italian Ministry of Health (Ricerca Corrente grant #RC201602G003692) to F.E.

Footnote: A.T. and A.D.F. contributed equally.

Disclosures: None declared.

Corresponding author:

Anna Taranta, PhD

Department of Nephrology and Urology, Division of Nephrology,
Bambino Gesù Children's Hospital

Viale San Paolo, 15,

00146, Rome, Italy.

Phone: +39 06 68592997

Fax: +39 06 68592904

email: anna.taranta@opbg.net

ACCEPTED MANUSCRIPT

Abstract

Cystinosis is a rare lysosomal storage disorder caused by loss of function mutations of the *CTNS* gene, encoding cystinosin, a symporter that mediates cystine efflux from lysosomes. About 95% of patients with cystinosis display renal Fanconi syndrome, short stature, osteopenia, and rickets. In this study, we investigated whether the absence of cystinosin primarily affects bone remodeling activity, apart from the influences of the Fanconi syndrome on bone mineral metabolism. Using micro-computed tomography, histomorphometric and bone serum biomarkers analysis, we evaluated the bone phenotype of one-month-old *ctns*^{-/-} (KO) male mice without tubulopathy. *In vitro* study was performed to characterize the effects of cystinosin deficiency on osteoblasts and osteoclasts. Micro-computed tomography analysis showed a reduction of trabecular bone volume, bone mineral density, number and thickness in KO mice compared to wild-type animals; histomorphometric analysis revealed a reduction of osteoblast and osteoclast parameters in tibias of cystinotic mice. Decreased levels of serum PINP and TRAcP in KO mice confirmed reduced bone remodeling activity. *In vitro* experiments showed an impairment of *ctns*^{-/-} osteoblasts and osteoclasts. In conclusion, cystinosin deficiency primarily affects bone cells, leading to a bone loss phenotype of KO mice, independent from renal failure.

Introduction

Cystinosis is a rare autosomal recessive disease caused by loss of function mutations of the *CTNS* gene, which encodes the cystinosin symporter.¹ Cystinosin is an integral lysosomal membrane protein responsible of proton-coupled cystine export from the lysosomal lumen to the cytosol.^{2, 3} Loss of cystinosin-dependent transport activity induces cystine accumulation in lysosomes, leading to crystals formation and cellular damage.⁴ Cystinosis is a monogenic disease. According to the severity of *CTNS* mutations, three major clinical presentations have been recognized, namely infantile or nephropathic, juvenile, and ocular non-nephropathic cystinosis.^{5, 6} Approximately 95% of patients suffer from nephropathic form, which manifests during the first year of life with renal Fanconi syndrome leading to excessive wasting of electrolytes and metabolites in the urine, growth retardation, osteopenia, and rickets.^{7, 8} Infants and young children with nephropathic cystinosis display skeletal abnormalities including genu valgum or varum, metaphyseal widening, rachitic rosary, frontal bossing, poor mobility, bone fractures, increased serum alkaline phosphatase level, hypocalcemia, hypophosphatemia, and hypokalemia.⁹⁻¹¹ To date, clinical manifestations associated with hypophosphatemic rickets in patients with nephropathic cystinosis, have been thought to be mainly caused by phosphate depletion, secondary to renal tubule damage.^{10, 12, 13} However, bone alterations and decreased mineralization described in an animal model of cystinosis were not associated with Fanconi syndrome.¹⁴ Moreover mesenchymal stem cells isolated from a patient with nephropathic cystinosis showed a reduced ability to differentiate into mature osteoblasts *in vitro*, thus independently from renal dysfunction.¹⁵ Taken together, these data suggest that other factors contribute to bone disease. To investigate whether skeletal alterations in nephropathic cystinosis are also due to primary bone defects, we have evaluated the effects of cystinosin deficiency in bone cells and the bone phenotype of *ctns*^{-/-} mice that have normal renal phenotype during the first post-natal month of life.

Materials and Methods

Animals

Mice were treated according to the NIH Guide for Care and Use of Laboratory Animals; Italian Legislative Decree 116/92; EEC Council Directive 86/609. C57BL/6 *ctns*^{-/-} mice were previously generated in the laboratory of Dr. Antignac, as described in Nevo et al.¹⁶

Blood and Urine analysis

Urine samples were collected from mice kept in metabolic cages for 24 hours. Urinary creatinine, glucose, albumin, calcium, and phosphate were measured by HITACHI Cobas C311 (Roche Diagnostiics GmbH, Mannheim, Germany). Clara Cell Protein (CC16) level was measured using Immunosorbent Assay kit in accordance with manufacturers' instructions (Biomatik, Wilmington, DE). Blood samples were taken from submandibular vein and collected in microtainer tubes (BD, Franklin Lakes, NJ) containing gel for serum separation. Creatinine and Blood Uric Nitrogen (BUN) were measured by HITACHI Cobas C311 (Roche Diagnostiics GmbH, Mannheim, Germany). Serum Calcium and Phosphate were evaluated by Siemens ADVIA 1800 Chemistry System (Siemens Healthineers, Erlangen, Germany). Tartrate-resistant acid phosphatase (TRAcP), carboxy-terminal collagen cross-links (CTX), procollagen type 1 amino-terminal propeptide (P1NP), parathyroid hormone 1-84 (PTH1-84), C-terminal fibroblast growth factor 23 (FGF23), and 1,25-dihydroxyvitamin D3 [1,25(OH)₂ Vit. D3] were measured by ELISA kits, according to the manufacturers' instructions (Biomedical Technologies Inc. Stoughton, MA, and Quidel, San Diego, CA).

Histology

Kidneys were fixed in 4% formaldehyde in 0.1 M phosphate buffer, pH 7.2, dehydrated in ethanol and processed for paraffin embedding. Three micron-thick sections were stained for megalin (Abcam,

Cambridge, UK) and cubilin (Santa Cruz, Saint Louis, MO) immunohistochemistry. For histological analysis of calcified tissue, bones were fixed in 4% formaldehyde in 0.1 M phosphate buffer, dehydrated in acetone, and embedded in 2-Hydroxyethyl-methacrylate. Histomorphometric measurements were performed on 2 to 3 μm -thick sections, with an interactive image analysis system (NIS-Elements BR 4.50.00). Nomenclature, symbols, and units of histomorphometric bone parameters were those suggested by the Histomorphometry Nomenclature Committee of the American Society for Bone and Mineral Research (ASBMR).¹⁷

Micro-CT

Femurs were excised and cleaned to remove soft tissues. A high-resolution desktop micro-tomographic imaging system ($\mu\text{CT}40$, Scanco Medical AG, Brüttisellen, Switzerland) was used to assess trabecular bone microarchitecture and cortical bone morphology in the distal femoral metaphysis and mid-diaphysis, respectively. Scans were acquired using a $10\ \mu\text{m}^3$ isotropic voxel size, 70 kVp peak x-ray tube intensity, 114 mA x-ray tube current, 200 ms integration time, and were subjected to Gaussian filtration and segmentation. Image acquisition and analysis protocols adhered to guidelines for the use of μCT for the assessment of bone microstructure in rodents.¹⁸ Trabecular bone was evaluated in a $1500\ \mu\text{m}$ long region (150 transverse slices) beginning $200\ \mu\text{m}$ above the peak of the distal growth plate and extending proximally. Trabecular bone was segmented from soft-tissue using a threshold of $388\ \text{mgHA}/\text{cm}^3$ and the Scanco Evaluation program Trabecular Morphology script was used to measure the trabecular bone volume fraction (BV/TV, %), trabecular thickness (Tb.Th, μm), trabecular number (Tb.N, $1/\text{mm}$), trabecular separation (Tb.Sp, μm), and trabecular bone mineral density (Tb.BMD, mgHA/cm^3). Cortical bone architecture was evaluated in a $500\ \mu\text{m}$ long region (50 transverse slices) at the femoral mid-diaphysis. Cortical bone was segmented using a threshold of $700\ \text{mgHA}/\text{cm}^3$ and then evaluated using the Scanco Mid-shaft Evaluation script to measure total cross-

sectional area (Tt.Ar, mm²), cortical bone area (Ct.Ar, mm²), medullary area (Ma.Ar, mm²), cortical bone area fraction (Ct.Ar/Tt.Ar, %), cortical thickness (Ct.Th, μm), as well as the maximum, minimum, and polar moments of inertia (Imax, Imin, and pMOI, mm⁴).

Cystine analysis

For cystine content measurements, kidney, long bones (ulna and radius), osteoblasts, and osteoclasts were sonicated in the presence of 10 mM N-ethylmaleimide. The protein fraction was precipitated by the addition of 10% 5-sulfosalicylic acid and measured using the Pierce bicinchoninic acid protein assay. Cystine levels were measured by high performance liquid chromatography (HPLC) as described in Pastore et al.¹⁹

Murine osteoblast primary cultures

Differentiation of bone marrow mesenchymal stem cells (MSC) into osteoblasts

MSC cells were isolated from bone marrow of wild-type mice. After reaching 90% confluence, cells were trypsinized and seeded in 12-well plates at a density of 8×10^4 cells/well. Medium supplemented with 10% FBS (Fetal Bovine Serum), 50 μg/mL L-ascorbic and 10 mM of β-glycerol phosphate (Sigma-Aldrich) was then added after 2 days. Medium was changed every three to four days and after 1, 2, and 3 weeks of culture gene expression analysis was performed. To confirm the osteogenic differentiation, alkaline phosphatase staining was evaluated by Alkaline Phosphatase activity kit No 86C (Sigma Aldrich, Saint Louis, MO).

Isolation of osteoblasts from calvaria

Calvaria were digested with *Chlostridium histolyticum* collagenase and trypsin at 37 °C three times for 15, 30, and 45 minutes, respectively, with gentle agitation. The isolated cells were grown in DMEM

plus 10% FBS, trypsinized, and plated according to the experimental protocol. ALP activity was evaluated as previously described.

Mineralization assay

Osteoblasts isolated from calvaria were cultured in DMEM plus 10% FBS, 10 mM β -glycerophosphate and 50 μ g/mL ascorbic acid to induce mineralization. After three weeks, Von Kossa staining was performed to evaluate mineralized area by image analysis system (NISElements BR 4.50.00)

Murine osteoclast primary cultures

Osteoclast precursors

Bone marrow of the long bones of mice was flushed out and diluted in Hank's solution. Cells were stratified over an equal volume of Histopaque 1077. After a centrifugation at 400 \times g for 30 min, the interface layer was isolated, washed twice in Hank's solution (250 \times g, 10 min), re-suspended in DMEM containing 10% FBS, and fixed in 4% formaldehyde after 3h. TRAcP activity was detected histochemically by Sigma-Aldrich kit No. 85 (Sigma Aldrich, Saint Louis, MO).

Osteoclast culture

For osteoclastogenesis, osteoclast precursors were cultured in DMEM plus 10% FBS supplemented with 50 ng/mL recombinant murine Macrophage-Colony Stimulating Factor (M-CSF) and 120 ng/mL recombinant murine Receptor Activator of Nuclear factor kappa-B Ligand (RANK-L) for 7 days. Osteoclasts were detected by histochemical staining for TRAcP.

Resorption assay

Osteoclast precursors were differentiated on bovine bone slices in DMEM plus 10% FBS supplemented with 50 ng/mL M-CSF 120 ng/mL RANK-L. Resorption pit area was measured by image analysis system (NISElements BR 4.50.00) and normalized for the osteoclast number.

Real time reverse transcription-PCR

Total RNA was extracted using the Trizol® procedure. One microgram of RNA was reverse transcribed using the Moloney murine leukemia virus reverse transcriptase. For real time PCR, 0.1 µg c-DNA, the Brilliant® SYBR® Green QPCR (Bioline, London, UK) master mix and primers indicated in Table 1 were used.

Statistics

Data were expressed as mean ± standard error of the mean (SEM) of at least three independent experiments or seven animals per group. Values were compared by unpaired *t* test if data pass normality tests (Kolmogorov-Smirnov, Shapiro-Wilk test) or by nonparametric Mann-Whitney test, as appropriate. A result with $P < 0.05$ was considered statistically significant. Analyses were performed through GraphPad Prism 6.

Results

Kidney phenotype

To study the primary role of bone in the development of osteopenia and rickets in the nephropathic cystinosis, skeletal alterations of *ctns*^{-/-} C57BL/6 mice (KO mice) were analyzed. Since cystinotic mice develop Fanconi syndrome between 2 and 9 months of age,¹⁶ the renal function was studied in male animals at different ages (1, 3, and 6 months). The first sign of renal damage was observed at three months of age and was characterized by urine loss of low molecular weight Clara cell protein (CC16). Glycosuria, normocalcemic hypercalciuria and hypophosphatemia developed at the age of six months,

whereas no changes of BUN, serum creatinine, diuresis, urinary phosphate, and albumin were revealed (Tables 2-3). 1,25(OH)₂ Vit. D3 levels did not show any alterations between wild-type (WT) and KO animals at different ages (Table 3).

Moreover, histological analysis of kidney biopsies isolated from 1-, 3-, and 6-month-old mice did not reveal the focal atrophy of juxta-glomerular proximal tubules ('swan neck' lesions), typical feature of nephropathic cystinosis (data not shown). In addition, the expression of two receptors (megalin and cubilin), whose decrease is a sign of tubular dysfunction, were evaluated. At one to three months of age KO mice did not show any differences in the expression of these receptors; reduced mRNA levels of megalin (*Irp2*) and a trend of decrease of cubilin were revealed in six-month-old *ctns*^{-/-} kidneys (Figure 1A-B). However, immunohistochemistry analysis did not display relevant alterations of the protein expression and localization of these two receptors (Figure 1C-D).

Cystine content

Cystinotic tissues are characterized by intra-lysosomal cystine accumulation. Cystine content was evaluated after animal sacrifice in kidneys and bones by HPLC. Cystine accumulated progressively in kidney (Figure 2A) and long bones (ulna and radius) (Figure 2B) of KO animals.

Bone phenotype in *ctns*^{-/-} mice

Bone phenotype was analyzed in 1-, 3- and 6-month-old animals. Micro-computed tomography showed a significant decrease in trabecular bone in the distal metaphysis of the femurs in 1-month-old cystinotic mice compared to wild-type animals (Table 4, Figure 3A). Concordantly, bone mineral density (BMD), bone volume (BV/TV), trabecular number (Tb.N), and thickness (Tb.Th) were significantly decreased, and trabecular separation (Tb.Sp) was increased (Table 4, Figure 3A, Supplementary Figure S1A). No significant differences were observed at later ages (Table 4, Figure

3B-C). Cortical bone was similar between WT and KO animals at 1 and 3 months and displayed significant reduction at 6 months (Table 5). Indeed, 6-month-old KO mice showed an obvious thinning of the collar micro-CT parameters with a reduction of maximum (Imax), minimum (Imin), and polar moments of inertia (pMOI) (Table 5).

High-power radiographs of tibia isolated from 1-month-old mice confirmed an osteopenic phenotype in growing cystinotic bones in the absence of renal damage (Supplementary Figure S1B).

Finally, PTH and FGF23 hormones regulating bone and kidney axis were evaluated. No statistically significant differences were observed between 1-month-old wild-type and cystinotic mice (Figure 4).

One-month-old *ctns*^{-/-} mice display decreased osteoblast activity

Osteoblasts and osteoclasts parameters were evaluated *in vivo* and *in vitro*

Semi-thin section of 1-month-old tibias stained with toluidine blue showed reduced surface occupied by osteoblasts, which were also reduced in number, in KO compared to WT animals (Figure 5A). Cystinotic osteoblasts also presented with scarce osteoid tissue (Figure 5A). This was confirmed by histomorphometric analyses (Figures 5B-C) and by lower serum levels of the bone formation marker P1NP (ng/mL; WT: 1130.0±120.1; KO: 931.6±114.6; $P = 0.004$) (Figure 5D). Moreover, reduced mRNA levels of the mature osteoblast markers alkaline phosphatase (*alp*) and type I collagen (*coll1a2*) (Figure 5E) were observed in KO femur samples. Conversely, no differences were revealed in the expression of the bone differentiation markers *runx2* (Runt-related transcription factor 2) and *sp7* (Osterix) (Figure 5E).

To evaluate if these alterations were directly caused by cystinosin deficiency in the osteoblast lineage, the expression of cystinosin was first evaluated in cultures of wild-type mesenchymal stem cells induced to differentiate into osteoblasts. The expression of cystinosin increased during osteoblast differentiation (Figure 6A). Further analyses showed that osteoblast cultures from *ctns*^{-/-} mice have

increased cystine content (Figure 6B) and decreased number of alkaline phosphatase (ALP) positive cells (Figure 6C-D). The expression of differentiation and activity markers was evaluated by quantitative-PCR and a reduced expression of *runx2*, *sp7*, *alp*, and *colla2* genes was observed (Figure 6E). Moreover, *in vitro* mineralization assays revealed reduced ability to release mineralized nodules of cystinotic osteoblasts compared to wild-type cells (Figure 6F-G).

One-month-old *ctns*^{-/-} mice display reduced osteoclastogenesis

To evaluate the involvement of osteoclasts in the osteopenic phenotype observed in KO animals, semi-thin sections of tibias from *ctns*^{-/-} mice were stained for the osteoclast-specific marker TRAcP. Reduced number of osteoclasts lining the trabecular bone of the proximal spongiosa was observed in KO mice (Figure 7A). This was confirmed by histomorphometric analyses showing a reduction in total osteoclast number (Oc.N/BS, N/mm²; WT: 16.8±4.2; KO: 7.7±6.1; *P* = 0.04) and surface (Oc.S/BS, %; WT: 22.5±6.6; KO: 12.9±4.9; *P* = 0.04) per bone surface (Figure 7B-C). Reduction of osteoclastogenesis was further confirmed by decreased TRAcP serum levels (Figure 7D). The measurement of the bone resorption marker CTX did not reveal any statistically significant alterations (ng/mL; WT: 36.0±9.5; KO: 30.6±3.4; *P* = 0.16). Finally, these findings were also supported by quantitative-PCR analysis showing reduced expression of osteoclast-specific genes, including receptor activator of nuclear factor κ B (*rank*) and matrix metalloproteinase 9 (*mmp9*) in 1 month-old KO femurs. No differences were revealed for cathepsin K (*ctsk*) and acid phosphatase 5 tartrate resistant (*acp5*) expression (Figure 7E).

To evaluate if these alterations were directly caused by cystinosis deficiency in the osteoclast lineage, the expression of cystinosis was studied in wild-type bone marrow macrophages, osteoclast precursors, and mature cells. A progressive increase of the *ctns* gene expression was observed during osteoclastogenesis (Figure 8A). After confirming accumulation of lysosomal cystine in KO osteoclasts

(Figure 8B), the effects of cystinosis deficiency were studied on osteoclast differentiation. The initial number of TRAP positive mononuclear precursors was similar in wild-type and cystinotic cultures (Figure 8C). After differentiation, a lower number of mature osteoclasts was observed in *ctns*^{-/-} cultures compared to wild-type cells (Figure 8D-E). These results were further confirmed by lower *acp5* expression in KO cultures compared to wild-type cells (Figure 8F). Furthermore, reduced ability to resorb bone was revealed in KO osteoclasts (Figure 8G-H).

Discussion

Bone complications are well known to physicians that manage patients with nephropathic cystinosis and may have substantial repercussion on linear growth and quality of life.²⁰ In patients with chronic renal failure, bone metabolism is impaired by complex interactions between kidneys, bone, and parathyroid glands that are primarily mediated by PTH, vitamin D, and FGF23, resulting in chronic kidney disease–mineral bone disorder (CKD-MBD). Skeletal defects in cystinosis have been attributed to the Fanconi syndrome, which causes metabolic acidosis, urinary leak of phosphate, impaired 1-alpha hydroxylation of vitamin D3, and loss of low-molecular weight proteins.²¹ High urinary loss of vitamin D3 binding protein may aggravate vitamin D3 deficiency.⁷ In addition, urinary copper wasting has also been proposed as a potential factor contributing to bone lesions in cystinosis, because copper is an essential co-factor promoting collagen lysine hydroxylation in bones.^{22, 23}

Cysteamine has represented a major advance in the cystine-depleting treatment of cystinosis.^{24, 25} This drug reacts with cystine generating mixed disulfides, which can exit the lysosome through other membrane transporters.^{26, 27} However, recent data suggest that cysteamine may be toxic at high concentrations, probably impairing collagen cross-linking; this effect may be amplified by copper deficiency.²² Patients with cysteamine toxicity develop skin lesions secondary to angioendotheliomatosis and in some cases develop abrupt bone deformities that can be confused with

rickets.²² In theory, these patients could represent the tip of the iceberg, and subtle bone defects secondary to cysteamine toxicity may contribute to bone lesions in many more patients with nephropathic cystinosis. In this view, high doses of cysteamine have been shown *in vitro* to inhibit osteoblast differentiation and mineralization.²⁸

Finally, bone lesions in nephropathic cystinosis may also be caused by a primary defect of bone cells. This was strongly suggested by observations made in the first reported mouse model of cystinosis that developed osteoporosis and rickets-like lesions in absence of renal failure and phosphate leak.¹⁴ This hypothesis is further supported by the observation of impaired osteogenic differentiation of mesenchymal stem cells isolated from bone marrow of a cystinotic patient.¹⁵ This defect was reversed by *in vitro* treatment with cysteamine.¹⁵

Here, it was first confirmed that cystinosin is expressed in bone and that cystine accumulates at high concentrations in this tissue. Animals were analyzed during the first six months of life. Differences in trabecular bone between mutated and wild-type animals were evident in the first month of life and disappeared progressively at later ages. Conversely, defects in cortical bone appeared at six months of age and could be associated with progressive cystine accumulation and the onset of kidney dysfunction. To confirm the first hypothesis, the effect of cysteamine should be tested, which was beyond the scope of the present study. In the clinical setting, patients well treated with cysteamine grow better,²⁹ supporting the hypothesis that cystine accumulation in bones has a deleterious effect.

Similarly to 6-month-old *ctns*^{-/-} animals, human subjects with chronic kidney failure have lower cortical density and higher cortical porosity in their long bones, without significant modification of bone trabecular parameters.³⁰ Hypothetically, incipient renal disease at six months may explain, at least in part, cortical defects observed at this age in *ctns*^{-/-} mice; indeed cortical bone loss could be due to

hyperparathyroidism frequently observed in CKD patients.³⁰ Accordingly, cystinotic teenagers and young adults with Fanconi syndrome display significant cortical impairment.³¹

Bone growth requires the sequential activation of bone cell maturation processes and constant remodeling. Children with nephropathic cystinosis display more growth retardation, compared to their classmates with the same degree of renal failure.³² This clinical observation further supports the hypothesis of an intrinsic bone defect in cystinosis, which is strongly corroborated by our results in 1-month-old cystinotic mice. At this age, which corresponds to maximal murine growth and bone formation rates,^{32, 33} animals had no signs of renal failure nor evidence of Fanconi syndrome. Yet, a significant reduction in trabecular bone volume that was not associated with differences in calciuria, phosphaturia, vitamin D3, PTH, and FGF23 compared to control animals was observed. Histomorphometric studies and low P1NP and TRAcP circulating levels provide clear evidence of low bone turnover, explaining the observed defects in trabecular bone. However it cannot be excluded that the alterations of bone phenotype observed in 1-month-old KO mice may be due to defective skeletal development. Embryonic and fetal development studies should be performed to identify alterations of skeletal morphogenesis.

The *in vitro* studies confirmed that cystinosin deficiency affects differentiation and activity of both osteoclasts and osteoblasts. Indeed KO osteoblasts showed a cell autonomous defect to mineralize. Although there is high variability among patients' skeletal alterations, a diffuse defective mineralization and scarce osteoblastic activity has been described in a patient's biopsy.⁹ Further studies are needed to evaluate whether reduced ability to mineralize could be related to impaired vesicles release and collagen deposition that could reflect the reduced osteoid surface in 1-month-old mice. Indeed a failure to secrete collagen has been reported in chondrocytes of a mouse model of lysosomal storage defect.³⁴ The impaired trafficking and the atypical clustering of lysosomes around perinuclear

area observed in cystinotic cells could explain how cystinosis deficiency affects osteoclast activity too.³⁵ For their resorbing activity osteoclasts need a tightly regulated trafficking of lysosomes and vesicles that release metalloproteinase 9 and cathepsin K in the bone resorption lacunae. An inhibition of the secretory machinery affects osteoclast function.³⁶ However, the reduced osteoclastogenesis observed in KO cultures was in contradiction with data obtained from Claramunt-Taberner and colleagues who demonstrated that patient mononuclear progenitors are more prone to generate osteoclasts than controls. However the authors showed that, even if cystinotic osteoclasts were increased in number, they were less active and cysteamine treatment further reduced their bone resorbing ability.²⁸ In agreement with these data, a strong reduction of the bone resorption activity was observed in KO osteoclasts. Taken together, these data provide evidence supporting the concept that bone growth is impaired in nephropathic cystinosis, independently from the Fanconi syndrome, chronic renal failure, and malnutrition. These defects were limited to the initial growth period, which corresponds approximately to pre- and early-school years in humans. At three months of age, no differences were observed between WT and KO animals. At this age, the rate of bone growth has already decreased substantially in mice,³² which probably explains lack of differences which are amplified only during periods of maximal growth. However, the spontaneous recovery of bone skeletal alterations was already documented in other genetic animal models. For example, the *ia/ia* incisor absent rat, showing an osteopetrotic phenotype due to *loss-of-function* of *plekhm1* [pleckstrin homology domain containing, family M (with RUN domain) member 1], developed a partial recovery of bone phenotype 30 to 50 days after birth.³⁷ The understanding of molecular and cellular alterations that occur in the skeleton during growth and adulthood could explain the changes of bone phenotype observed in these transgenic animal models.

Acknowledgments

We thank the Center for Skeletal Research Core, Massachusetts General Hospital for the microCT analysis and Professor Corinne Antignac who provided C57BL/6 cystinotic and wild-type mice.

A.T. and A.D.F. designed the study. G.B., M.R., M.D., G.D.G., and L.R.R. performed experiments. A.T., A.D.F., F.E., A.P., and O.P. analyzed data. A.T., A.D.F., N.N., and F.E. interpreted data. A.T., A.D.F., and F.E. wrote the manuscript. F.E., O.P., and A.P. revised the manuscript. A.T. is the guarantor of this work and, as such, had full access to all of the data in the study and takes responsibility for the integrity of the data and the accuracy of the data analysis.

REFERENCES

- [1] Town M, Jean G, Cherqui S, Attard M, Forestier L, Whitmore SA, Callen DF, Gribouval O, Broyer M, Bates GP, van't Hoff W, Antignac C: A novel gene encoding an integral membrane protein is mutated in nephropathic cystinosis. *Nature genetics* 1998, 18:319-24.
- [2] Kalatzis V, Cherqui S, Antignac C, Gasnier B: Cystinosis, the protein defective in cystinosis, is a H(+)-driven lysosomal cystine transporter. *The EMBO journal* 2001, 20:5940-9.
- [3] Ruivo R, Anne C, Sagne C, Gasnier B: Molecular and cellular basis of lysosomal transmembrane protein dysfunction. *Biochimica et biophysica acta* 2009, 1793:636-49.
- [4] Wilmer MJ, Emma F, Levtchenko EN: The pathogenesis of cystinosis: mechanisms beyond cystine accumulation. *American journal of physiology Renal physiology* 2010, 299:F905-16.
- [5] Emma F, Nesterova G, Langman C, Labbe A, Cherqui S, Goodyer P, Janssen MC, Greco M, Topaloglu R, Elenberg E, Dohil R, Trauner D, Antignac C, Cochat P, Kaskel F, Servais A, Wuhl E, Niaudet P, Van't Hoff W, Gahl W, Levtchenko E: Nephropathic cystinosis: an international consensus document. *Nephrology, dialysis, transplantation : official publication of the European Dialysis and Transplant Association - European Renal Association* 2014, 29 Suppl 4:iv87-94.
- [6] Ivanova E, De Leo MG, De Matteis MA, Levtchenko E: Cystinosis: clinical presentation, pathogenesis and treatment. *Pediatric endocrinology reviews : PER* 2014, 12 Suppl 1:176-84.
- [7] Elmonem MA, Veys KR, Soliman NA, van Dyck M, van den Heuvel LP, Levtchenko E: Cystinosis: a review. *Orphanet journal of rare diseases* 2016, 11:47.
- [8] Sakarcan A: The Fanconi syndrome of cystinosis: insights into the pathophysiology. *The Turkish journal of pediatrics* 2002, 44:279-82.

- [9] Bacchetta J, Greco M, Bertholet-Thomas A, Nobili F, Zustin J, Cochat P, Emma F, Boivin G: Skeletal implications and management of cystinosis: three case reports and literature review. *BoneKEY reports* 2016, 5:828.
- [10] Sirrs S, Munk P, Mallinson PI, Ouellette H, Horvath G, Cooper S, Da Roza G, Rosenbaum D, O'Riley M, Nussbaumer G, Hoang LN, Lee CH: Cystinosis with sclerotic bone lesions. *JIMD reports* 2014, 13:27-31.
- [11] Florenzano P, Ferreira C, Nesterova G, Roberts MS, Tella SH, de Castro LF, Brown SM, Whitaker A, Pereira RC, Bulas D, Gafni RI, Salusky IB, Gahl WA, Collins MT: Skeletal Consequences of Nephropathic Cystinosis. *J Bone Miner Res* 2018.
- [12] Gahl WA, Thoene JG, Schneider JA: Cystinosis. *The New England journal of medicine* 2002, 347:111-21.
- [13] Klusmann M, Van't Hoff W, Monsell F, Offiah AC: Progressive destructive bone changes in patients with cystinosis. *Skeletal radiology* 2013.
- [14] Cherqui S, Sevin C, Hamard G, Kalatzis V, Sich M, Pequignot MO, Gogat K, Abitbol M, Broyer M, Gubler MC, Antignac C: Intralysosomal cystine accumulation in mice lacking cystinosin, the protein defective in cystinosis. *Molecular and cellular biology* 2002, 22:7622-32.
- [15] Conforti A, Taranta A, Biagini S, Starc N, Pitisci A, Bellomo F, Cirillo V, Locatelli F, Bernardo ME, Emma F: Cysteamine treatment restores the in vitro ability to differentiate along the osteoblastic lineage of mesenchymal stromal cells isolated from bone marrow of a cystinotic patient. *Journal of translational medicine* 2015, 13:143.
- [16] Nevo N, Chol M, Bailleux A, Kalatzis V, Morisset L, Devuyst O, Gubler MC, Antignac C: Renal phenotype of the cystinosis mouse model is dependent upon genetic background. *Nephrology Dialysis Transplantation* 2010, 25:1.

- [17] Dempster DW, Compston JE, Drezner MK, Glorieux FH, Kanis JA, Malluche H, Meunier PJ, Ott SM, Recker RR, Parfitt AM: Standardized nomenclature, symbols, and units for bone histomorphometry: a 2012 update of the report of the ASBMR Histomorphometry Nomenclature Committee. *Journal of bone and mineral research : the official journal of the American Society for Bone and Mineral Research* 2013, 28:2-17.
- [18] Bouxsein ML, Boyd SK, Christiansen BA, Guldberg RE, Jepsen KJ, Muller R: Guidelines for assessment of bone microstructure in rodents using micro-computed tomography. *Journal of bone and mineral research : the official journal of the American Society for Bone and Mineral Research* 2010, 25:1468-86.
- [19] Pastore A, Massoud R, Motti C, Lo Russo A, Fucci G, Cortese C, Federici G: Fully automated assay for total homocysteine, cysteine, cysteinylglycine, glutathione, cysteamine, and 2-mercaptopropionylglycine in plasma and urine. *Clinical chemistry* 1998, 44:825-32.
- [20] Besouw M, Levtchenko E: Growth retardation in children with cystinosis. *Minerva pediatrica* 2010, 62:307-14.
- [21] Nesterova G, Gahl WA: Cystinosis. *GeneReviews*(R). Edited by Adam MP, Ardinger HH, Pagon RA, Wallace SE, Bean LJH, Stephens K, Amemiya A. Seattle (WA): University of Washington, Seattle
University of Washington, Seattle. GeneReviews is a registered trademark of the University of Washington, Seattle. All rights reserved., 1993.
- [22] Besouw MT, Schneider J, Janssen MC, Greco M, Emma F, Cornelissen EA, Desmet K, Skovby F, Nobili F, Lilien MR, De Paepe A, Malfait F, Symoens S, van den Heuvel LP, Levtchenko EN: Copper deficiency in patients with cystinosis with cysteamine toxicity. *The Journal of pediatrics* 2013, 163:754-60.
- [23] Langman CB: Bone Complications of Cystinosis. *The Journal of pediatrics* 2017, 183s:S2-s4.

- [24] Langman CB, Greenbaum LA, Grimm P, Sarwal M, Niaudet P, Deschenes G, Cornelissen EA, Morin D, Cochat P, Elenberg E, Hanna C, Gaillard S, Bagger MJ, Rioux P: Quality of life is improved and kidney function preserved in patients with nephropathic cystinosis treated for 2 years with delayed-release cysteamine bitartrate. *The Journal of pediatrics* 2014, 165:528-33.e1.
- [25] Al-Hemidan A, Shoughy SS, Kozak I, Tabbara KF: Efficacy of topical cysteamine in nephropathic cystinosis. *The British journal of ophthalmology* 2017, 101:1234-7.
- [26] Allison SJ: Therapy: An extended-release form of cysteamine bitartrate for cystinosis. *Nature reviews Nephrology* 2012, 8:374.
- [27] Brodin-Sartorius A, Tete MJ, Niaudet P, Antignac C, Guest G, Ottolenghi C, Charbit M, Moysse D, Legendre C, Lesavre P, Cochat P, Servais A: Cysteamine therapy delays the progression of nephropathic cystinosis in late adolescents and adults. *Kidney international* 2012, 81:179-89.
- [28] Claramunt-Taberner D, Flammier S, Gaillard S, Cochat P, Peyruchaud O, Machuca-Gayet I, Bacchetta J: Bone disease in nephropathic cystinosis is related to cystinosis-induced osteoclastic dysfunction. *Nephrology, dialysis, transplantation : official publication of the European Dialysis and Transplant Association - European Renal Association* 2018.
- [29] Kleta R, Bernardini I, Ueda M, Varade WS, Phornphutkul C, Krasnewich D, Gahl WA: Long-term follow-up of well-treated nephropathic cystinosis patients. *The Journal of pediatrics* 2004, 145:555-60.
- [30] Nickolas TL, Stein EM, Dworakowski E, Nishiyama KK, Komandah-Kosseh M, Zhang CA, McMahon DJ, Liu XS, Boutroy S, Cremers S, Shane E: Rapid cortical bone loss in patients with chronic kidney disease. *Journal of bone and mineral research : the official journal of the American Society for Bone and Mineral Research* 2013, 28:1811-20.
- [31] Bertholet-Thomas A, Claramunt-Taberner D, Gaillard S, Deschênes G, Sornay-Rendu E, Szulc P, Cohen-Solal M, Pelletier S, Carlier MC, Cochat P, Bacchetta J. Teenagers and young adults with

nephropathic cystinosis display significant bone disease and cortical impairment. *Pediatr Nephrol.* 2018, 33:1165-72.

[32] Van Stralen KJ, Emma F, Jager KJ, Verrina E, Schaefer F, Laube GF, Lewis MA, Levtchenko EN: Improvement in the renal prognosis in nephropathic cystinosis. *Clinical journal of the American Society of Nephrology: CJASN* 2011, 6:2485-91.

[33] Stratikopoulos E, Szabolcs M, Dragatsis I, Klinakis A, Efstratiadis A. The hormonal action of IGF1 in postnatal mouse growth. *Proc Natl Acad Sci U S A.* 2008, 105:19378-83.

[34] Bartolomeo R, Cinque L, De Leonibus C, Forrester A, Salzano AC, Monfregola J, De Gennaro E, Nusco E, Isabella Azario I, Lanzara C, Serafini M, Levine B, Ballabio A, Settembre C. mTORC1 hyperactivation arrests bone growth in lysosomal storage disorders by suppressing autophagy. *Journal of Clinical Investigation* 2017, 127:3717-29.

[35] Ivanova EA, De Leo MG, Van Den Heuvel L, Pastore A, Dijkman H, De Matteis MA, Levtchenko EN. Endo-lysosomal dysfunction in human proximal tubular epithelial cells deficient for lysosomal cystine transporter cystinosin. *PLoS One* 2015, 10:e0120998.

[36] Del Fattore A, Teti A, Rucci N. Bone cells and the mechanisms of bone remodelling. *Front Biosci (Elite Ed).* 2012, 4:2302-21.

[37] Van Wesenbeeck L, Odgren PR, Coxon FP, Frattini A, Moens P, Perdu B, MacKay CA, Van Hul E, Timmermans JP, Vanhoenacker F, Jacobs R, Peruzzi B, Teti A, Helfrich MH, Rogers MJ, Villa A, Van Hul W. Involvement of PLEKHM1 in osteoclastic vesicular transport and osteopetrosis in incisors absent rats and humans. *Journal of Clinical Investigation* 2007, 117:919-30.

Figure Legends

Figure 1. Megalin and cubilin expression in kidneys of wild-type and cystinotic mice. **A-B:** Real time reverse transcription-PCR for megalin (*lrp2*) (**A**) and cubilin (*cbln*) (**B**) was performed on cDNA obtained from mRNA extracted from kidney of wild-type (WT, black column) and cystinotic (KO, white column) mice at 1, 3, and 6 months of age. Values are normalized vs the housekeeping gene *gapdh*. Results are mean±SEM. * $P < 0.05$ vs wild-type animals. **C-D:** Immunohistochemistry in paraffin-embedded 3- μ m-thick renal sections of 1-, 3-, and 6-month-old (1 m, 3 m, and 6 m) wild-type and cystinotic mice. Staining for megalin (**C**) and cubilin (**D**). Original magnification 10X.

Figure 2. Cystine content in kidney and bone of wild-type and cystinotic mice. High-performance liquid chromatography measurement of cystine levels in kidneys (**A**) and long bones (ulna and radius) (**B**) of wild-type (WT, black column) and cystinotic (KO, white column) mice at 1, 3, and 6 months of age. * $P < 0.05$, ** $P < 0.005$ vs wild-type animals.

Figure 3. Micro-CT analysis. Representative micro-CT images of distal femurs of wild-type (WT) and cystinotic (KO) mice at 1 (**A**), 3 (**B**), and 6 (**C**) months of age.

Figure 4. PTH and FGF23 levels in 1-month-old mice. Elisa assay for PTH1-84 (**A**) and FGF23 (**B**) in plasma samples from wild-type (WT) and cystinotic (KO) mice.

Figure 5. *In vivo* effects of cystinosin deficiency on osteoblasts in 1-month-old mice. A: Representative images of toluidine blue-stained semi-thin sections of wild-type (WT) and cystinotic (KO) proximal spongiosa lined by cuboidal osteoblasts (white arrows). Original magnification 20X. **B-C:** Histomorphometric evaluation of osteoblast surface and osteoid surfaces in proximal spongiosa tibia of wild-type (WT, black column) and cystinotic (KO, white column) mice. **D:** ELISA assay for P1NP in serum collected from WT and KO mice. **E:** Gene expression of osteoblast markers (*runx2*, *sp7*, *alp*, and *colla2*) measured by real time reverse transcription-PCR analysis on mRNA extracted from femurs of wild-type and cystinotic mice. Values are normalized vs the housekeeping gene *gapdh*. * $P < 0.05$; ** $P < 0.005$ vs wild-type animals.

Figure 6. *In vitro* osteoblast analysis. A: Real time reverse transcription-PCR analysis for cystinosin (*ctns*) in wild-type stromal mesenchymal stem cells (t0) and MSC stimulated to differentiate in osteoblasts for 7, 14, and 21 days. *ctns* values are normalized vs the housekeeping gene *gapdh*. **B:** HPLC measurement of cystine levels in osteoblasts isolated from wild-type (WT, black column) and cystinotic (KO, white column) mice. **C:** *In vitro* osteoblasts isolated from skull bone of WT and KO mice were monitored by alkaline phosphatase (ALP) staining. Original magnification 4X. **D:** Quantitative expression of ALP positive cells in wild-type and cystinotic cultures. Results are reported as percentage (%) vs wild-type osteoblasts. **E:** Real time reverse transcription-PCR expression analysis on RNA extracted from wild-type and cystinotic osteoblasts for *runx2*, *sp7*, *alp*, and *colla2*. Values are normalized vs the housekeeping gene *gapdh*. **F:** Osteoblasts isolated from WT and KO mice were induced to form mineralized nodules and monitored by Von Kossa staining. Original magnification 10X. **G:** Quantitative analysis of mineralized area in WT and KO cultures. Values are reported as percentage (%) vs wild-type osteoblasts activity. * $P < 0.05$ vs wild-type cells.

Figure 7. *In vivo* effects of cystinosin deficiency on osteoclasts in 1-month-old mice. A: Histochemical detection of the osteoclast-specific marker TRAcP in the semi-thin sections of proximal spongiosa from wild-type (WT) and cystinotic (KO) tibias. Original magnification 20X. **B-C:** Histomorphometric analysis of osteoclast number and osteoclast surface per bone surface in wild-type (WT, black column) and cystinotic (KO, white column) mice. **D:** ELISA assay for TRAcP in serum collected from wild-type and cystinotic mice. **E:** Real time reverse transcription-PCR expression analysis on RNA extracted from femurs using primer pairs and conditions specific for *rank*, *mmp9*, *ctsk*, and *acp5*. Values are normalized vs the housekeeping gene *gapdh*. * $P < 0.05$; ** $P < 0.005$ vs wild-type animals.

Figure 8. *In vitro* osteoclast analysis. A: Real time reverse transcription-PCR analysis for cystinosin in wild-type bone marrow macrophage cells (BMM), osteoclast precursors (pOc), and mature osteoclasts (Oc). **B:** HPLC measurement of cystine levels in osteoclasts isolated from wild-type (WT, black column) and cystinotic (KO, white column) mice. **C:** Bone marrows were isolated from WT and KO animals, fixed after 3 h and stained for TRAcP to quantify osteoclast mononuclear precursors. **D:** Representative pictures of TRAcP positive osteoclast cultures obtained from BMM cultured in the presence of M-CSF and RANK-L to induce osteoclastogenesis. Original magnification 10X. **E:** Quantification of TRAcP positive multinucleated (>3 nuclei) cells. **F:** Real time reverse transcription-PCR expression analysis on RNA extracted from WT and KO osteoclast cultures using primer pairs and conditions specific for *acp5*. Values are normalized vs the housekeeping gene *gapdh*. **G:** Representative pictures of blue toluidine-stained bone sections showing resorption lacunae (white arrows) obtained from WT and KO osteoclasts. Original magnification 10X. **H:** Quantification of

resorbed area in WT and KO cultures. Values are normalized for osteoclast number. Results are reported as percentage (%) vs wild-type osteoclasts activity. * $P < 0.05$; ** $P < 0.005$ vs wild-type cells.

ACCEPTED MANUSCRIPT

Table 1. List and sequence of primers.

Gene	Forward Primer	Reverse Primer
<i>lrp2</i>	5' CAGTGGATTGGGTAGCAGGA 3'	5' GCTTGGGGTCAACAACGATA 3'
<i>cbln</i>	5' TCATTGGCCTCAGACATTCC 3'	5' CCCAGACCTTCACAAAGCTG 3'
<i>runx2</i>	5' CCCAGCCACCTTTACCTACA 3'	5' TATGGAGTGCTGCTGGTCTG 3'
<i>sp7</i>	5' ACCTTTCGTCTTCCTGAGCTT 3'	5' CTGGCGCATAGGGGTAAAGT 3'
<i>alp</i>	5' GGACAGGACACACACACA 3'	5' CAAACAGGAGAGCCACTTCA 3'
<i>col1a2</i>	5' CCGTGCTTCTCAGAACATCA 3'	5' GAGCAGCCATCGACTAGGAC 3'
<i>rank</i>	5' CACTTAGGCAGTAGGCC 3'	5' ACTCTTCTTCTTAACTGTGAGGCA 3'
<i>mmp9</i>	5' TGAATCAGCTGGCTTTTGTG 3'	5' GTGGATAGCTCGGTGGTGT 3'
<i>ctsk</i>	5' GTAGCCACGCTTCCTATCCG 3'	5' CCTCCAGGTTATGGGCAGAG 3'
<i>acp5</i>	5' GAGAACGGTGTGGGCTATGT- 3'	5' CTGTGGGATCAGTTGGTGTG 3'
<i>gapdh</i>	5' GTTCCTACCCCAATGTGT 3'	5' GTGAGGGAGATCCTCAGTG 3'

Table 2. Urine chemistry in wild-type (WT) and cystinotic (KO) mice.

	1 month		3 months		6 months	
	WT	KO	WT	KO	WT	KO
CC16 ($\mu\text{g/g creatinine}$)	285 \pm 72	350 \pm 54	26 \pm 6	60 \pm 10**	20 \pm 6	1166 \pm 751*
Albumin (mg/g creatinine)	20.1 \pm 4.2	13.0 \pm 5.4	4.4 \pm 0.4	4.5 \pm 0.8	17.1 \pm 3.9	15.3 \pm 2.4
Creatinine (mg/dL)	49.7 \pm 4.4	42.8 \pm 9.0	48.5 \pm 3.6	44.5 \pm 6.5	44.0 \pm 4.9	47.3 \pm 3.8
Glucose (mM)	7.2 \pm 1.0	8.2 \pm 1.7	3.1 \pm 0.2	3.0 \pm 0.8	0.9 \pm 0.3	15.0 \pm 3.7**
Calcium (mg/mg creatinine)	0.41 \pm 0.07	0.71 \pm 0.14	0.16 \pm 0.01	0.42 \pm 0.20	0.13 \pm 0.02	0.34 \pm 0.14*
Phosphate (mg/mg creatinine)	3.09 \pm 0.44	3.51 \pm 0.48	3.20 \pm 0.25	2.40 \pm 0.39	2.23 \pm 0.50	2.34 \pm 0.39
Diuresis (mL/24h)	0.60 \pm 0.10	0.68 \pm 0.14	0.93 \pm 0.16	0.91 \pm 0.11	1.87 \pm 0.36	1.21 \pm 0.14

Each group is composed of more than seven mice. KO mice were compared to age-matched WT mice for statistical analysis. Values are reported as means \pm SEM. Mann Whitney test. * $P < 0.05$, ** $P < 0.005$ vs WT mice.

ACCEPTED MANUSCRIPT

Table 3. Serum chemistry in WT and KO mice.

	1 month		3 months		6 months	
	WT	KO	WT	KO	WT	KO
BUN (mg/dL)	29.8±1.5	32.5±2.4	45.4±1.4	39.4±3.1	65.3±4.9	59.3±6.8
Creatinine (mg/dL)	0.58±0.11	0.83±0.16	1.15±0.04	1.22±0.06	1.32±0.03	1.85±0.19
Calcium (mg/dL)	9.66±0.23	10.4±0.44	9.04±0.18	9.54±0.21	9.63±0.24	9.61±0.32
Phosphate (mg/dL)	11.6±0.7	9.9±0.6	8.7±0.7	7.9±0.3	8.8±0.2	7.8±0.4*
1.25(OH)₂ Vit. D3 (pmol/L)	261±41	182±16	332±58	299±22	219±4	259±30

Values are reported as mean±SEM. Mann Whitney test. * $P < 0.05$ vs WT mice.

BUN, Blood Urea Nitrogen.

Table 4. Microarchitectural parameters of femurs from WT and KO mice.

	1 month		3 months		6 months	
	WT	KO	WT	KO	WT	KO
BMD (mgHA/cm³)	189±9	163±8**	230±22	233±36	194±35	182±22
BV/TV (%)	16.0±0.1	12.7±1.1**	18.2±2.6	19.4±3.6	13.1±3.9	11.7±2.5
Tb.N (1/mm)	4.50±0.26	3.56±0.42**	5.11±0.20	5.23±0.53	3.73±0.35	3.66±0.32
Tb.Th (µm)	43.60±0.55	41.00±0.82***	52.00±2.50	52.10±2.34	57.40±4.54	54.00±3.02
Tb.Sp (µm)	230±10	300±40**	188±9	186±23	262±27	268±31
Conn.D (1/mm³)	293±29.5	244±27.7	189±17.2	203±47.8	71.6±27.7	69.2±19.6
SMI	1.86±0.05	1.99±0.14	1.90±0.22	1.75±0.30	2.21±0.44	2.28±0.35

Each group is composed of more than seven mice. Values are reported as mean \pm SEM. Mann Whitney test. ** $P < 0.005$; *** $P < 0.001$ vs WT mice.

BV/TV, Bone Volume Fraction; BMD, Bone Mineral Density; Tb.N, Trabecular Number; Tb.Th, Trabecular Thickness; Tb.Sp, Trabecular Separation; Conn.D, Connectivity Density; SMI, Structural Model Index.

ACCEPTED MANUSCRIPT

Table 5. Microarchitectural parameters of mid-diaphysis of femurs from WT and KO mice.

	1 month		3 months		6 months	
	WT	KO	WT	KO	WT	KO
Tt.Ar (mm²)	1.58±0.16	1.43±0.13	1.85±0.15	1.91±0.12	2.06±0.19	1.85±0.16*
Ct.Ar (mm²)	0.40±0.03	0.38±0.02	0.80±0.05	0.81±0.05	0.86±0.07	0.77±0.04**
Ma.A (mm²)	1.17±0.13	1.05±0.11	1.04±0.11	1.09±0.07	1.20±0.15	1.07±0.12
Ct.Ar/Tt.Ar (%)	25.7±1.7	26.6±1.5	43.6±1.7	42.6±0.7	41.8±3.3	42.1±1.1
Ct.Th (µm)	91.0±2.0	89.4±1.2	179.7±2.6	175.1±2.3	178.6±4.8	170.0±1.4*
Imax (mm⁴)	0.11±0.02	0.09±0.02	0.26±0.04	0.28±0.04	0.31±0.05	0.26±0.04*
Imin (mm⁴)	0.07±0.01	0.06±0.01	0.13±0.02	1.75±0.30	0.16±0.03	0.12±0.02*

pMOI (mm⁴)	0.18±0.03	0.15±0.02	0.39±0.06	0.41±0.05	0.47±0.08	0.38±0.06*
------------------------------	-----------	-----------	-----------	-----------	-----------	------------

Values are reported as mean±SEM. Mann Whitney test. * $P < 0.05$; ** $P < 0.005$ vs WT mice.

Tt.Ar, Total Area; Ct.Ar, Bone Area; Ma.A, Medullary Area; Ct.Ar/Tt.Ar, Bone Area Fraction; Ct.Th, Cortical Thickness; I_{max}, maximum moment of inertia; I_{min}, minimum moment of inertia; pMOI, polar moment of inertia.

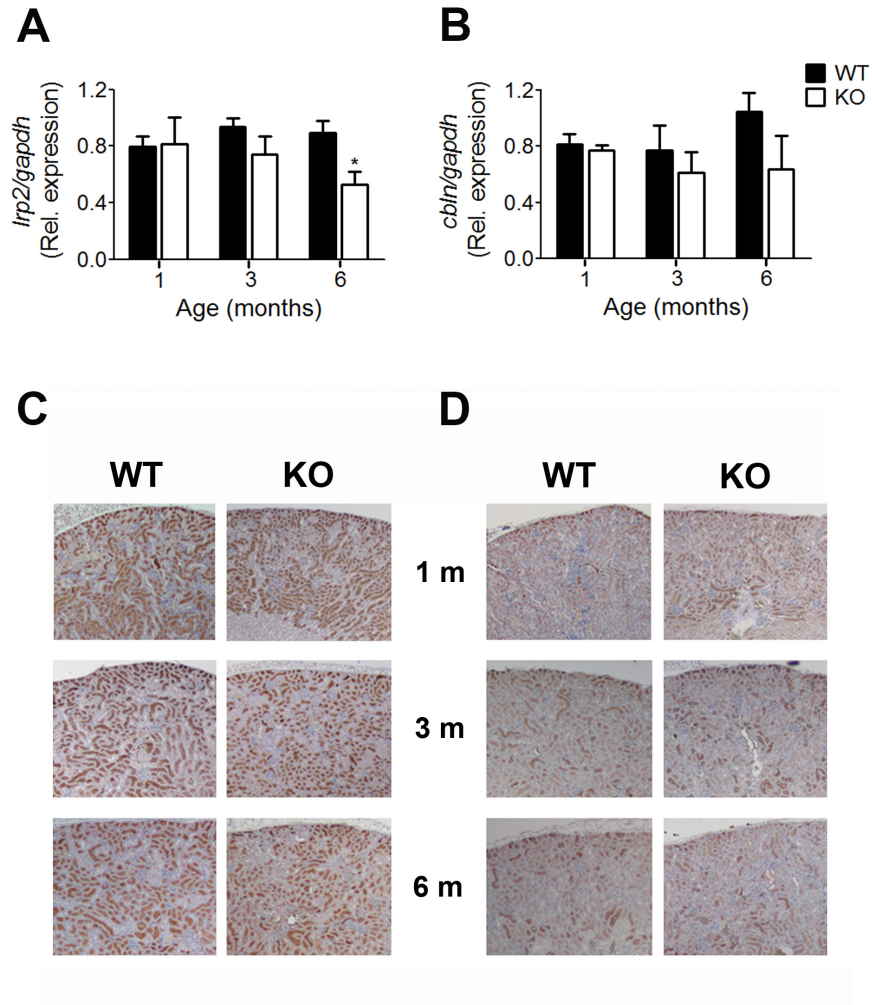


Figure 1

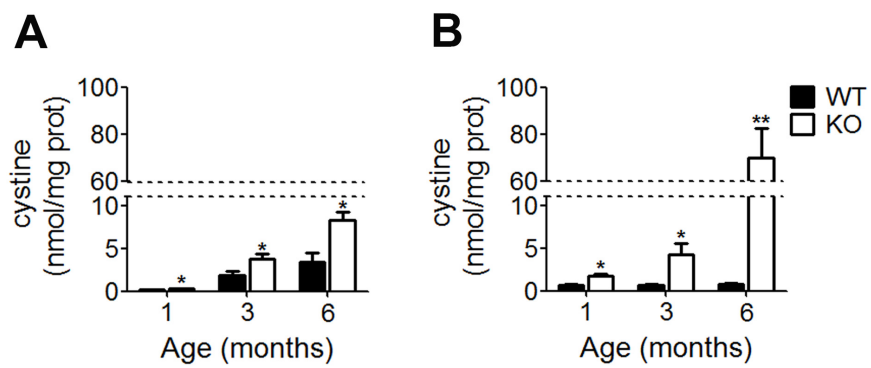


Figure 2

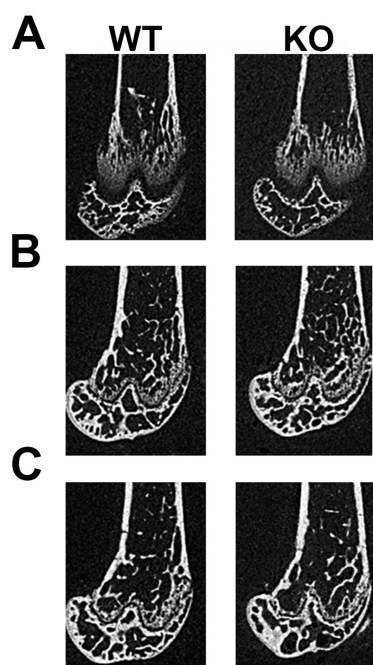


Figure 3

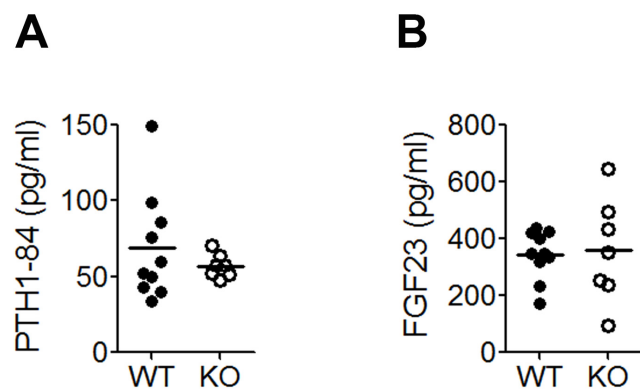


Figure 4

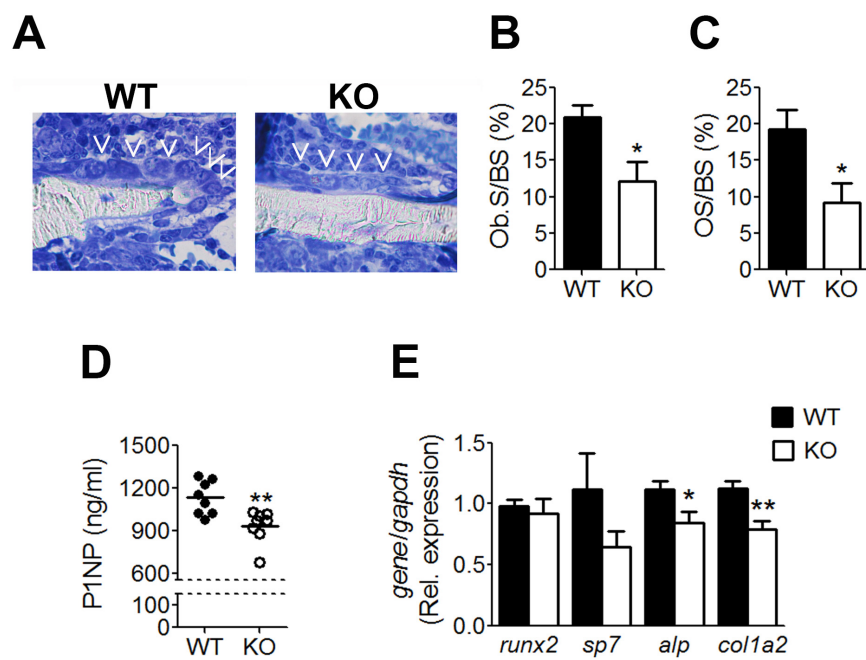
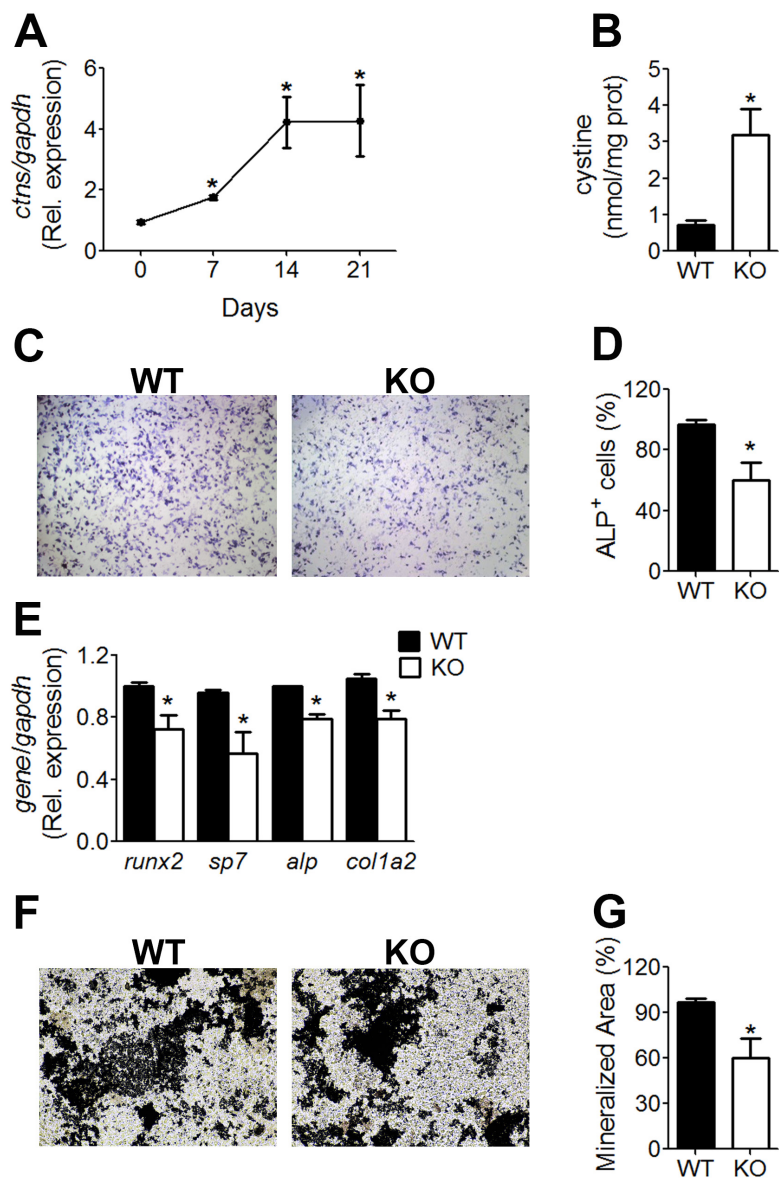


Figure 5



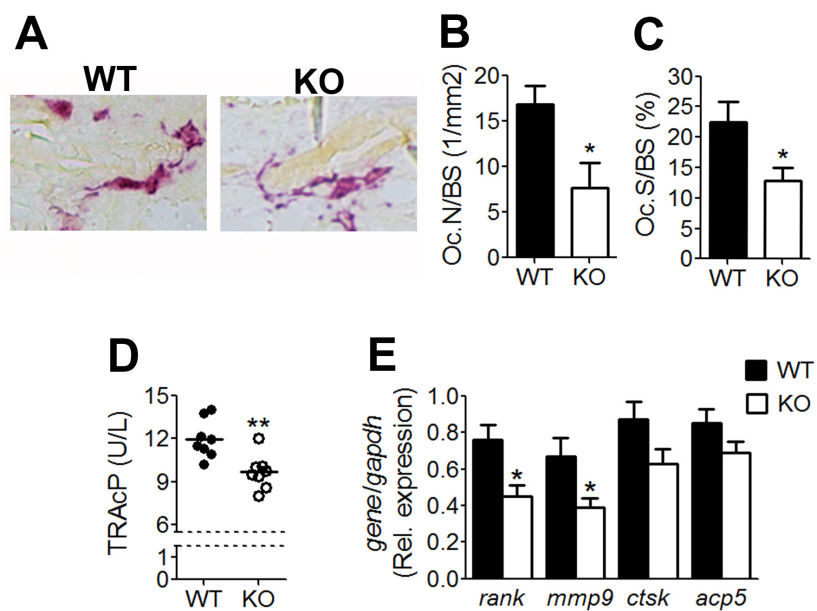


Figure 7

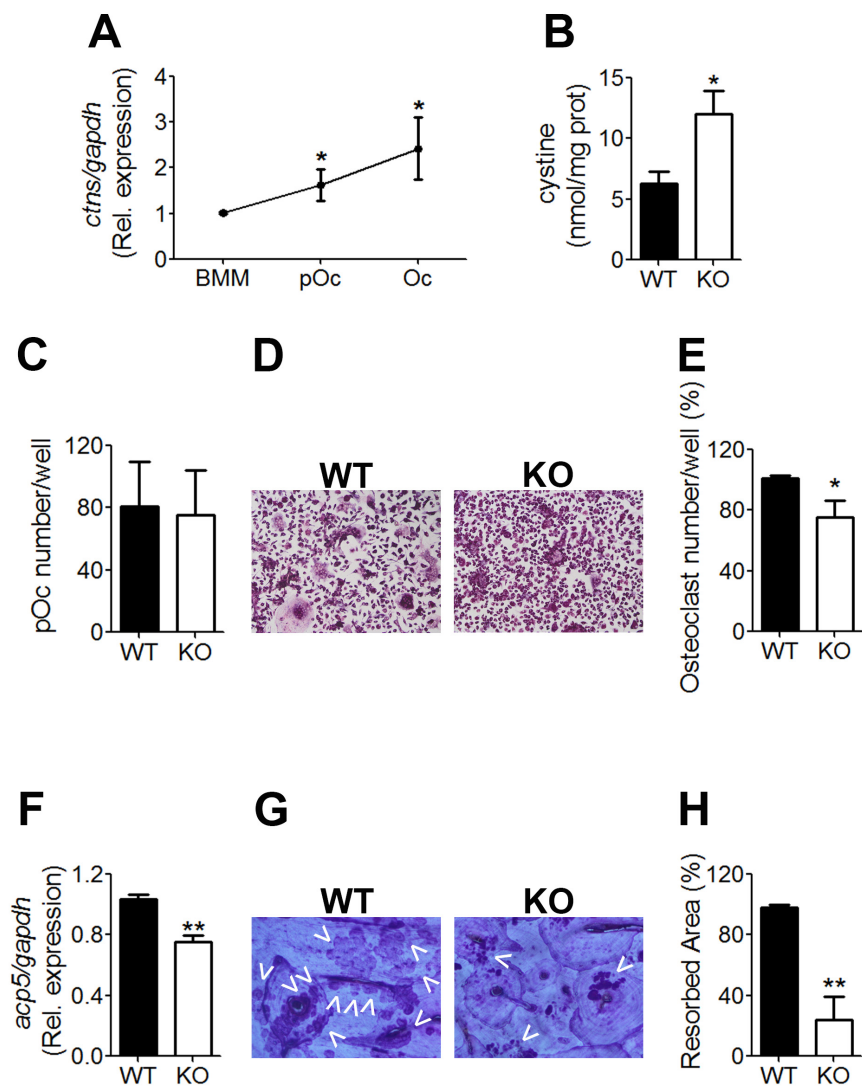


Figure 8